Journal of Engineering Mathematics **28**: 227–240, 1994.

A method of domain decomposition for calculating the steady flow past a cylinder

S.J.D. D'ALESSIO and S.C.R. DENNIS

University of Western Ontario, Department of Applied Mathematics, London, Ontario, Canada N6A 5B7

Received 19 March 1993; accepted in revised form 9 September 1993

Abstract. For flow past a cylinder it is known that the vorticity is only significant in a thin boundary-layer adjacent to the surface and within a parabolic wake far from the cylinder. To address this behaviour of the vorticity a numerical method is implemented whereby the flow field is decomposed into two regions: an inner region to deal with boundary-layer phenomena and an outer region to model wake phenomena. This method equally applies to any cylinder cross section. The equations of motion are solved in each region and are matched at the boundary. Numerical solutions have been carried out for the trial case of a circular cylinder and the agreement with existing results is good.

1. Introduction

The steady flow of a viscous incompressible fluid past a circular cyclinder has received much attention. Numerical work on this problem includes that of Thom [1], Kawaguti [2], Keller and Takami [3], Takami and Keller [4], Dennis and Chang [5, 6], Nieuwstadt and Keller [7], Dennis [8] and Fornberg [9] to mention a few. One of the major difficulties encountered in obtaining accurate numerical solutions of the Navier–Stokes equations lies in the behaviour of the vorticity as illustrated in Fig. 1. When the equations are expressed in terms of the modified polar co-ordinates (ξ, θ), where $\xi = \ln(r/a)$ and a is the radius of the cylinder, the vorticity is concentrated in a thin boundary-layer on the surface of thickness $\xi = O(1/\sqrt{R})$ and within a diminishing wake far from the cylinder having a width $\theta = O(e^{-\xi/2}/\sqrt{R})$. A further complication is the fact that the boundary-layer and wake thicknesses depend on the Reynolds number, R.

One approach of accommodating the vorticity behaviour would be to utilize grid reduction. In the far wake, grid reduction in the θ direction must be implemented, whereas

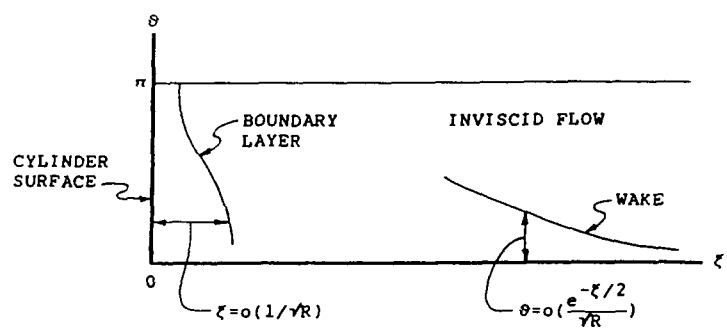

Fig. 1. The flow field for $\theta \geq 0$ in modified polar co-ordinates.

near the cylinder the boundary-layer warrants grid reduction in the ξ direction. Young [10] introduced a successful technique of performing grid reduction in the far wake. He chose to halve the grid size in the θ direction within the wake each time the breadth of the wake diminished by a factor of two. This leaves the same number of grid points in the wake region. Wherever a grid reduction was initiated, interpolation was used to obtain values at the new grid points on the half grid. As many as three grid reductions were undertaken for moderate Reynolds numbers.

In the present method domain decomposition is used. The flow field is divided into two regions: an inner region dealing with boundary-layer phenomena and an outer region designed to model wake phenomena. The idea of decomposing the flow field into two regions was proposed by Dennis [8]. In the outer region a change of co-ordinate variables suggested by the asymptotic solution of Imai [11] is introduced. We let

$$z = e^{-\xi/2} \tag{1}$$

$$\phi = \frac{\sqrt{R}e^{\xi/2}\theta}{2\sqrt{2}} = \frac{\theta}{2kz}, \tag{2}$$

where

$$k = \sqrt{\frac{2}{R}}. \tag{3}$$

Advantages of working in terms of these variables are two fold. Firstly, the otherwise infinite interval (ξ^*, ∞) of ξ is now mapped to the finite interval $(z^*, 0)$ with $z^* = \exp(-\xi^*/2)$ denoting the boundary separating the two regions. This allows the entire flow field to be considered, which is seldom done in computational fluid dynamics. Secondly, the breadth of the wake remains constant throughout the outer region by this choice of the variable ϕ. This is equivalent to stretching the narrowing wake and can be viewed as an analytical analog of the grid reduction done by Young [10]. Consequently though, the finite range $(-\pi, \pi)$ of θ also gets stretched to the interval $(-\pi/2kz, \pi/2kz)$ and tends to the infinite interval (∞, ∞) of ϕ as $z \to 0$. This technique is illustrated in Fig. 2 for the symmetrical case.

The boundary separating the two regions given by $\xi = \xi^*$ (or $z = z^*$) is permitted to move

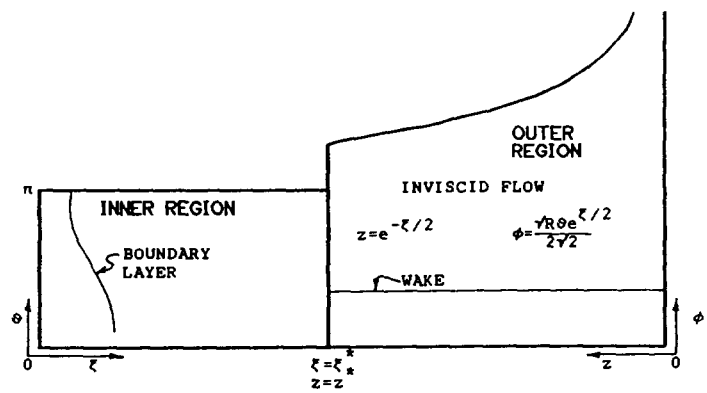

Fig. 2. Domain decomposition of the flow field.

according to the Reynolds number. Allowing this provides the necessary grid reduction in the boundary-layer. Two formulae specifying its movement are given by

$$\xi^* = \xi_0^* \sqrt{\frac{R_0}{R}} \tag{4}$$

$$\xi^* = \xi_0^* - \ln\left(\frac{R}{R_0}\right). \tag{5}$$

In the above, ξ_0^* corresponds to the location of the boundary for some Reynolds number R_0. Equation (4) is based on boundary-layer theory as evidenced by the factor $1/\sqrt{R}$ while (5) is suggested by wake theory.

The method is explained in detail in the following sections. Our main object is to describe the basic mathematical analysis underlying the method. This is illustrated with numerical tests which employ the well-known example of flow past a circular cylinder. However, the method can be extended to a cylinder of any cross section. The results obtained are at low Reynolds numbers, but they illustrate all the basic processes. In effect the method is a numerical matching procedure of inner and outer type solutions.

2. Basic equations and boundary conditions

In terms of the modified polar co-ordinates (ξ, θ) the equations of motion in dimensionless form involving the stream function ψ and the vorticity ζ are

$$\frac{\partial^2 \psi}{\partial \xi^2} + \frac{\partial^2 \psi}{\partial \theta^2} + e^{2\xi}\zeta = 0 \tag{6}$$

$$\frac{\partial^2 \zeta}{\partial \xi^2} + \frac{\partial^2 \zeta}{\partial \theta^2} = \frac{R}{2}\left(\frac{\partial \psi}{\partial \theta}\frac{\partial \zeta}{\partial \xi} - \frac{\partial \psi}{\partial \xi}\frac{\partial \zeta}{\partial \theta}\right), \tag{7}$$

where the Reynolds number R is based on the diameter of the cylinder and is given by $R = 2aU/\nu$. Here, U is the uniform incoming stream and ν the kinematic viscosity.

For symmetric flow the solutions of (6) and (7) are required in the semi-infinite rectangular strip bounded by $\xi \geqslant 0$, $0 \leqslant \theta \leqslant \pi$ and are subject to the boundary conditions

$$\psi = \frac{\partial \psi}{\partial \xi} = 0 \quad \text{for } \xi = 0, \tag{8}$$

$$e^{-\xi}\frac{\partial \psi}{\partial \xi} \to \sin\theta, \qquad e^{-\xi}\frac{\partial \psi}{\partial \theta} \to \cos\theta, \quad \zeta \to 0 \qquad \text{as } \xi \to \infty, \tag{9}$$

$$\psi = \zeta = 0 \quad \text{for } \theta = 0, \pi. \tag{10}$$

In the event of asymmetric flow resulting from a rotating circular cylinder, condition (8) is replaced by

$$\psi = 0, \qquad \frac{\partial \psi}{\partial \xi} = -\Omega \quad \text{for } \xi = 0, \tag{11}$$

where Ω denotes the dimensionless angular velocity and is related to the dimensional angular velocity ω according to $\Omega = 2a\omega/U$. Periodicity is also used instead of (10), namely

$$\psi(\xi, \theta) = \psi(\xi, \theta + 2\pi), \qquad \zeta(\xi, \theta) = \zeta(\xi, \theta + 2\pi) \tag{12}$$

and the equations are to be solved in the region $\xi \geqslant 0$, $-\pi \leqslant \theta \leqslant \pi$.

3. Formulation in outer region

The mathematical details associated with the transformation (1)–(3) will now be addressed. In the variables (z, ϕ) the vorticity transport equation (7), after omitting the term $\partial^2\zeta/\partial\xi^2$ and approximating $\sin\theta = \sin(2\phi kz) \sim 2\phi kz$ and $\cos\theta \sim 1 + O(k^2z^2)$ for small z, takes on the form

$$\frac{\partial^2\zeta}{\partial\phi^2} + \left(2\phi - \frac{z^2}{k}\frac{\partial\psi^*}{\partial z}\right)\frac{\partial\zeta}{\partial\phi} + \left(2 + \frac{z}{k}\frac{\partial\psi^*}{\partial\phi}\right)z\frac{\partial\zeta}{\partial z} = 0\,. \tag{13}$$

Here, ψ^* refers to the perturbed stream function and is related to ψ by

$$\psi = \psi^* + \mathrm{e}^{\xi}\sin\theta = \psi^* + \frac{1}{z^2}\sin(2\phi kz)\,. \tag{14}$$

The justification of the approximations made in arriving at (13) will be discussed later. It is worth noting that all the non-linearities present in the Navier–Stokes equations are preserved in (13).

By considering the limiting solution of (13) as $z \to 0$, Dennis [12] suggested an alternative method for obtaining the asymptotic solution. In this limit (13) reduces to

$$\frac{\partial^2\zeta}{\partial\phi^2} + 2\phi\frac{\partial\zeta}{\partial\phi} + 2z\frac{\partial\zeta}{\partial z} = 0\,, \tag{15}$$

and by separation of variables has fundamental solutions

$$\zeta_n = -A_n z^{n+1}\mu_n(\phi)\,, \quad n = 0, 1, 2, \ldots, \tag{16}$$

where the functions $\mu_n(\phi)$ are defined by

$$\mu_n(\phi) = \frac{1}{\sqrt{2^n n!\sqrt{\pi}}}\,\mathrm{e}^{-\phi^2/2}\,H_n(\phi)\,, \tag{17}$$

$H_n(\phi)$ being the Hermite polynomials. The functions $\mu_n(\phi)$ are orthogonal in the interval $(-\infty, \infty)$ and are normalized so that

$$\int_{-\infty}^{\infty}\mu_n^2\,\mathrm{d}\phi = 1\,.$$

In order for ζ to have the proper behaviour as $z \to 0$ we must have that $A_0 = 0$. Thus, the leading term of the series becomes

$$\zeta \sim -A_1 z^2\mu_1(\phi)\,, \tag{18}$$

where the constant A_1 is related to the drag coefficient C_D through

$$A_1 = \frac{C_D R}{4\sqrt{2}\pi^{1/4}}. \tag{19}$$

For small z, (18) is in complete agreement with Imai [11].

The limit point solutions (16) reveal that it is natural for the vorticity to be expanded in a Hermite series in the outer region. Acting on this suggestion, we expand ζ in the asymptotic series

$$\zeta(z, \phi) = -A_1 z^2 \, \mathrm{e}^{-\phi^2/2} \sum_{n=1}^{\infty} g_n(z)\mu_n(\phi). \tag{20}$$

The effect of this is to scale the vorticity and eliminate the dependence on ϕ by reducing (13) to a set of ordinary differential equations given by

$$g_n' - \frac{(n-1)}{z} g_n = F_n(z), \quad n = 1, 2, \ldots, \tag{21}$$

where the prime denotes differentiation with respect to z and the non-linear right-hand side, $F_n(z)$, is

$$F_n(z) = -\sum_{i=1}^{\infty} \left\{ \frac{g_i}{k} \int_{-\infty}^{\infty} \frac{\partial \psi^*}{\partial \phi} \mu_n \mu_i \, \mathrm{d}\phi + \sqrt{\frac{i+1}{2}} \frac{z g_i}{k} \int_{-\infty}^{\infty} \frac{\partial \psi^*}{\partial z} \mu_n \mu_{i+1} \, \mathrm{d}\phi \right.$$
$$\left. + \frac{z g_i'}{2k} \int_{-\infty}^{\infty} \frac{\partial \psi^*}{\partial \phi} \mu_n \mu_i \, \mathrm{d}\phi \right\}, \quad n = 1, 2 \ldots. \tag{22}$$

The parabolic nature of the problem in the far field is apparent by the resulting first-order differential equations (21). These equations are subject to the conditions

$$g_n(0) = -\delta_{1,n}, \quad n = 1, 2, \ldots, \tag{23}$$

where

$$\delta_{m,n} = \begin{cases} 0 & \text{if } m \neq n \\ 1 & \text{if } m = n \end{cases}. \tag{24}$$

Young [10], using a perturbative method, generated series solutions for the system of differential equations (21) which are valid for small z.

The stream function equation (6) expressed in terms of ψ^* and the variables (z, ϕ) becomes

$$\frac{\partial^2 \psi^*}{\partial \phi^2} = -4A_1 k^2 \, \mathrm{e}^{-\phi^2/2} \sum_{n=1}^{\infty} g_n(z)\mu_n(\phi). \tag{25}$$

Here, we have neglected the term $\partial^2 \psi^* / \partial \xi^2$. This equation can be integrated twice using the properties of Hermite polynomials. For the case of symmetrical flow only odd solutions are permissable and we impose the conditions

$$\psi^*(z, 0) = \psi^*\left(z, \frac{\pi}{2kz}\right) = 0. \tag{26}$$

The asymptotic series for the perturbed stream function in the outer region then becomes

$$\psi^*(z,\phi) = \sqrt{2}\pi^{1/4}A_1k^2g_1(z)\left(\operatorname{erf}(\phi) - \frac{2kz}{\pi}\phi\right) - 2A_1k^2\,\mathrm{e}^{-\phi^2/2}\sum_{n=3}^{\infty}\frac{g_{2n-3}(z)\mu_{2n-5}(\phi)}{\sqrt{(2n-3)(2n-4)}} \tag{27}$$

where $\operatorname{erf}(\phi)$ designates the error function defined by

$$\operatorname{erf}(\phi) = \frac{2}{\sqrt{\pi}}\int_0^{\phi}\mathrm{e}^{-x^2}\,\mathrm{d}x\,. \tag{28}$$

For asymmetric flow we invoke the condition of periodicity

$$\psi^*\left(z,-\frac{\pi}{2kz}\right) = \psi^*\left(z,\frac{\pi}{2kz}\right) \tag{29}$$

and set the remaining arbitrary function of z which can be added to $\psi^*(z,\phi)$ equal to $-(C_L/\pi)\ln z$ as suggested by Imai [11]. Here, C_L denotes the lift coefficient. This yields

$$\psi^*(z,\phi) = \sqrt{2}\pi^{1/4}A_1k^2g_1(z)\left(\operatorname{erf}(\phi) - \frac{2kz}{\pi}\phi\right) - 2A_1k^2\,\mathrm{e}^{-\phi^2/2}\sum_{n=2}^{\infty}\frac{g_n(z)\mu_{n-2}(\phi)}{\sqrt{n(n-1)}} - \frac{C_L}{\pi}\ln z\,. \tag{30}$$

It is clear that (30) simplifies to (27) when $C_L = 0$ and when n is odd. Also, in obtaining (27) and (30) the approximations $\operatorname{erf}(\pi/2kz) = 1$ and $\exp(-\pi^2/8k^2z^2)\mu_{n-2}(\pi/2kz) = 0$ were used. It is interesting to point out that although ψ^* is continuous at $\phi = \pm\pi/2kz$ in (30), $\partial\psi^*/\partial\phi$ and $\partial\psi^*/\partial z$ are not. Similarly, although $\psi^* = 0$ at $\phi = \pi/2kz$ in (27), $\partial\psi^*/\partial z$ is not zero. These, however, pose no difficulty since they only appear in the integrals given by (22) where they are multiplied by exponential factors present in the functions $\mu_n(\phi)$. The exponential decay is given by $\exp(-\phi^2)$ and is responsible for damping out any discrepancies. Lastly, for small z, (27) reduces to

$$\psi^*(z,\phi) \sim \frac{C_D}{2}\left(\frac{2kz\phi}{\pi} - \operatorname{erf}(\phi)\right) \tag{31}$$

while (30) collapses to

$$\psi^*(z,\phi) \sim \frac{C_D}{2}\left(\frac{2kz\phi}{\pi} - \operatorname{erf}(\phi)\right) - \frac{C_L}{\pi}\ln z\,, \tag{32}$$

both of which are in full agreement with the results of Imai [11].

4. Method of solution for symmetric flow

We begin by discretizing the computational domain. The inner region bounded by $0 \leqslant \xi \leqslant \xi^*$, $0 \leqslant \theta \leqslant \pi$ is reduced to a network of $(N+1)\times(M+1)$ grid points situated at

$$\xi_i = ih\,,\quad i = 0, 1, \ldots, N \tag{33}$$

$$\theta_j = jk\,, \quad j = 0, 1, \ldots, M\,, \tag{34}$$

where

$$h = \xi^*/N \tag{35}$$

$$k = \pi/M\,. \tag{36}$$

In the outer region the interval $(0, z^*)$ is divided into $L+1$ equally spaced points given by

$$z_i = ih_z\,, \quad i = 0, 1, \ldots, L \tag{37}$$

with

$$h_z = z^*/L\,. \tag{38}$$

The method used to solve the governing equations for the case of a stationary cylinder is an extension of the Dennis and Chang [5, 6] technique accommodating the outer region.

In the inner region, the stream function equation (6) is reduced to a set of ordinary differential equations by expanding ψ in the sine series

$$\psi(\xi, \theta) = \sum_{n=1}^{\infty} f_n(\xi) \sin n\theta \tag{39}$$

which automatically satisfies (10). Thus, (6) now becomes

$$f_n'' - n^2 f_n = -r_n(\xi)\,, \quad n = 1, 2, \ldots, \tag{40}$$

where the prime denotes differentiation with respect to ξ and $r_n(\xi)$ is defined by

$$r_n(\xi) = \frac{2\,\mathrm{e}^{2\xi}}{\pi} \int_0^{\pi} \zeta \sin n\theta \, \mathrm{d}\theta\,, \quad n = 1, 2, \ldots. \tag{41}$$

Boundary conditions for f_n can be obtained from (8)–(9) and are given by

$$f_n(0) = f_n'(0) = 0\,, \tag{42}$$

$$\mathrm{e}^{-\xi} f_n' \to \delta_{1,n}\,, \qquad \mathrm{e}^{-\xi} f_n \to \delta_{1,n} \quad \text{as } \xi \to \infty\,. \tag{43}$$

The differential equations (40) are solved by a marching algorithm employing Filon quadrature. The details can be found in Dennis and Chang [5].

The vorticity transport equation (7) is solved by finite differences using the scheme developed by Dennis [13] to ensure diagonal dominance. The surface vorticity can be determined by inverting (41) and evaluating it at $\xi = 0$. This yields the expression

$$\zeta(0, \theta) = \sum_{n=1}^{\infty} r_n(0) \sin n\theta\,. \tag{44}$$

Along the boundary $\xi = \xi^*$ the gradient condition based on the asymptotics is used in the form

$$\zeta(\xi^*, \theta) = \zeta(\xi^* - h, \theta)\, \mathrm{e}^{-h/2} \exp\left[-\frac{R}{4} \mathrm{e}^{\xi^*}(1 - \mathrm{e}^{-h})(1 - \cos\theta)\right]. \tag{45}$$

To complete the solution procedure for ζ, another condition is necessary. This can be obtained from the properties of the solutions of (40) and involve integrals given by

$$\int_0^\infty e^{-n\xi} r_n(\xi)\, d\xi = -2\delta_{1,n}\,, \quad n = 1, 2, \ldots . \tag{46}$$

These integral conditions are exact and span the entire flow field from the cylinder surface to infinity. They are appropriate conditions to use in this method because the whole flow field is considered. They also play an important role in linking the inner and outer regions together and can be rewritten as

$$\int_0^{\xi^*} e^{-n\xi} r_n(\xi)\, d\xi + 2\int_0^{z^*} z^{2n-1} r_n(z)\, dz = -2\delta_{1,n}\,, \quad n = 1, 2, \ldots . \tag{47}$$

Expressed this way, the contribution from each region is apparent.

In the outer region, using a sine series expansion for ψ^* proves to be inadequate owing to its limiting sawtooth behaviour. Instead, the asymptotic series (27) is used. The vorticity is found by solving the set of equations given by (21). These differential equations are integrated using a step-by-step procedure based on Filon integration and the trapezoidal approximation. The stable direction of integration of these equations is in the negative z direction from $z = z^*$ to $z = 0$. Initial conditions at $z = z^*$ are provided by decomposing the vorticity at the edge of the inner region into a Hermite series. By means of this we obtain

$$g_n(z^*) = \frac{1}{A_1 k z^{*3}\sqrt{2^n n!\sqrt{\pi}}} \int_0^\pi \zeta(\xi^*, \theta) H_n\left(\frac{\theta}{2kz^*}\right) d\theta\,, \quad \text{for } n \text{ odd}\,. \tag{48}$$

This procedure can be tested by comparing the values resulting at $z = 0$ against the exact theoretical ones given by (23).

Lastly, the expressions for $r_n(z)$ are

$$r_n(z) = \frac{2A_1 k}{\pi z} \sum_{i=1}^{\infty} \frac{g_i(z)}{\sqrt{2^i i!\sqrt{\pi}}} \int_{-\infty}^{\infty} e^{-\phi^2} H_i(\phi) \sin(2nkz\phi)\, d\phi\,, \quad n = 1, 2, \ldots . \tag{49}$$

In arriving at the above, the limits of integration $-\pi/2kz$, $\pi/2kz$ were justifiably and conveniently set to $-\infty$, ∞, respectively. The numerical solution of (21) requires knowledge of $r_n(0)$ and $F_n(0)$. Using the asymptotic solutions, the analytical expressions

$$r_n(0) = -\frac{nC_D}{\pi}\,, \quad n = 1, 2, \ldots \tag{50}$$

$$F_n(0) = \begin{cases} (-1)^{\frac{n+1}{2}} \dfrac{C_D\sqrt{R}}{2\sqrt{\pi}} \dfrac{\sqrt{n!}}{2^n\left(\dfrac{n-1}{2}\right)!} & \text{for } n \text{ odd} \\ -\dfrac{C_L\sqrt{R}}{\sqrt{2\pi}}\delta_{n,2} & \text{for } n \text{ even} \end{cases} \tag{51}$$

can be derived.

The computational procedure can now be discussed. After all infinite summations have

been replaced by a finite number of terms and initial guesses supplied for a given R, then the following steps are repeated until convergence on the drag coefficient is reached:

1. Calculate $r_n(\xi)$ for $n = 1, 2, \ldots, N_0$ in the inner region except at $\xi = 0$ and $r_n(z)$ for $n = 1, 2, \ldots, N_0$ throughout the outer region.
2. Determine $r_n(0)$ for $n = 1, 2, \ldots, N_0$ by enforcing the integral conditions and in doing so compute the surface vorticity from (44); moderate under-relaxation must be applied.
3. Calculate ζ throughout the inner region by finite differences.
4. Solve the differential equations (21) for $g_n(z)$, $n = 1, 2, \ldots, N_1$ to get the vorticity in the outer region.
5. Repeat steps (1) to (4) a specified number of times.
6. Solve the differential equations (40) for $f_n(\xi)$, $n = 1, 2, \ldots, N_0$ to get ψ in the inner region and update the expression for $\psi^*(z, \phi)$ in the outer region.
7. Compute C_D and check whether convergence is reached; this completes one cycle of the procedure.

Step (5) represents an inner iteration allowing for the fact that the equation for ζ is nonlinear and must be solved iteratively. Hence, it converges much more slowly than the linear Poisson equation for ψ which is solved during each cycle of the procedure.

5. Extension to asymmetric flow

For asymmetric flow past a rotating circular cylinder the computational domain is discretized as before with the exception that $-\pi \leqslant \theta \leqslant \pi$ and

$$\theta_j = jk\,, \quad j = -M, \ldots, M\,. \tag{52}$$

Because the method of Dennis and Chang [5, 6] has not yet been successfully extended to deal with steady asymmetrical flow, the equations of motion (6)–(7) are solved entirely by finite-differences in the inner region using a Gauss–Seidel iterative procedure. The surface vorticity is computed by a second-order finite-difference expression derived by taking a Taylor series expansion of ψ about the cylinder surface and making use of both conditions (11) for ψ. This expression is given by

$$\zeta(0, \theta) = \left\{ -\frac{1}{3}\left(4\zeta(h, \theta) - \zeta(2h, \theta)\right) - \frac{4\psi(h, \theta)}{h^2} - \frac{4\Omega}{h} \right\} \Big/ \left(1 + \frac{4h}{3}\right). \tag{53}$$

After sweeping through all $(N + 1) \times (2M + 1)$ grid points a specified number of times, the drag and lift coefficients are updated and inserted wherever necessary.

In the outer region ψ^* is known from (30) and is responsible for coupling the two regions as do the integral conditions in the symmetrical case. The vorticity, ζ, is found by solving the differential equations (21) subject to the initial condition at $z = z^*$

$$g_n(z^*) = \frac{1}{2A_1 k z^{*3} \sqrt{2^n n! \sqrt{\pi}}} \int_{-\pi}^{\pi} \zeta(\xi^*, \theta) H_n\left(\frac{\theta}{2kz^*}\right) \mathrm{d}\theta\,, \quad n = 1, 2, \ldots. \tag{54}$$

It must be remembered that in the case of asymmetrical flow all n in (21) must be retained.

This then enables $F_n(z)$ given by (22) to be updated. Convergence on the drag and lift coefficients to a specified accuracy was adopted as the criterion for termination of the procedures.

6. Results

Numerical solutions for symmetric flow were obtained for the range $1 \leq R \leq 40$. It became more difficult to obtain convergence of the iterative procedures for higher R. This can be explained by the observation that at around $R = 40$ the optimum position of the boundary separating the two regions approaches the wake bubble. The vorticity behaves differently inside the bubble from outside and the Hermite series is less satisfactory in representing the vorticity there regardless of the number of terms retained. Constantly pushing the boundary outside the growing wake bubble only provokes other problems resulting from the singular nature of the vorticity as $z = 0$ is approached.

It was found that (5) was the more appropriate formula to govern the movement of the boundary $\xi = \xi^*$. The use of (4) suffered from the drawback that the boundary moved in too rapidly. After numerous trial runs the following parameter values were used: $\xi_0^* = 4$, $R_0 = 5$, $N \times M = 70 \times 60$ and $L = 20$. Other parameter values are listed in Table 1, where N_0 and N_1 denote the number of terms in the sine and Hermite series respectively and ω refers to the relaxation parameter. With the number of terms shown in Table 1, the Hermite series reproduced the vorticity at the edge of the inner region to five decimal places. Although we have used the series truncation method we could equally have solved equation (13) by numerical methods using a step-by-step procedure to advance the solution in the z direction. However, the goal of the present work is to uncover the basic mathematical structure of the far-field flow and to find an effective method of dealing with it as is done by the series truncation method.

Numerical results and flow properties are documented in Table 2. Here, $P_0(0)$ and $P_0(\pi)$ refer to the rear and front stagnation point pressures, respectively. The pressure coefficient is defined by

$$P_0(\theta) = 1 + \frac{4}{R}\int_{-\pi}^{\theta}\left(\frac{\partial\zeta}{\partial\xi}\right)_0 \mathrm{d}\theta + 2\int_0^{\infty}\left(\frac{2}{R}\frac{\partial\zeta}{\partial\theta} + \zeta\frac{\partial\psi}{\partial\xi}\right)\mathrm{d}\xi\,, \tag{55}$$

and the drag and lift values are given by

$$C_D = \frac{2}{R}\int_{-\pi}^{\pi}\left(\frac{\partial\zeta}{\partial\xi} - \zeta\right)_0 \sin\theta\,\mathrm{d}\theta\,; \qquad C_L = \frac{2}{R}\int_{-\pi}^{\pi}\left(\zeta - \frac{\partial\zeta}{\partial\xi}\right)_0 \cos\theta\,\mathrm{d}\theta\,. \tag{56}$$

Table 1. Parameters used in the calculations

R	N_0	N_1	ω
1	20	5	0.05
5	20	5	0.05
10	20	10	0.05
20	30	10	0.05
30	30	10	0.05
40	40	15	0.025

Table 2. Comparisons with existing results

R	Authors	C_D	$P_0(0)$	$P_0(\pi)$	l_w	θ_s
1	Present	10.29	−2.693	3.918	–	–
	Takami and Keller (1969)	10.28	−2.719	3.905	–	–
	Nieuwstadt and Keller (1973)	10.31	−2.928	3.730	–	–
5	Present	3.894	−0.887	1.839	–	–
	Dennis and Chang (1970)	4.116	−1.044	1.872	–	–
10	Present	2.719	−0.623	1.477	0.519	29.1°
	Takami and Keller (1969)	2.750	−0.670	1.474	0.500	29.3°
	Dennis and Chang (1970)	2.846	−0.742	1.489	0.53	29.6°
	Nieuwstadt and Keller (1973)	2.828	−0.692	1.500	0.434	28.0°
20	Present	1.969	−0.540	1.264	1.775	43.2°
	Takami and Keller (1969)	2.024	−0.555	1.264	1.844	43.7°
	Dennis and Chang (1970)	2.045	−0.589	1.269	1.88	43.7°
	Nieuwstadt and Keller (1973)	2.053	−0.582	1.274	1.786	43.4°
	Fornberg (1980)	2.000	−0.54	1.28	1.82	–
30	Present	1.673	−0.544	1.185	3.055	49.0°
	Takami and Keller (1969)	1.717	−0.530	1.184	3.223	49.6°
	Nieuwstadt and Keller (1973)	1.733	−0.556	1.177	3.086	49.4°
40	Present	1.451	−0.488	1.142	4.323	52.5°
	Takami and Keller (1969)	1.524	−0.512	1.141	4.650	53.6°
	Dennis and Chang (1970)	1.522	−0.509	1.144	4.69	53.8°
	Nieuwstadt and Keller (1973)	1.550	−0.554	1.117	4.357	53.3°
	Fornberg (1980)	1.498	−0.46	1.14	4.48	–

Also, l_w denotes the wake length measured from the rear of the cylinder to the end of the separated region and θ_s refers to the angle of separation where the surface vorticity vanishes.

As previously mentioned, several approximations in arriving at (13) and (25) were made. These include the neglect of the terms $\partial^2\zeta/\partial\xi^2$ and $\partial^2\psi^*/\partial\xi^2$ and the retaining of only one term in the expansion for $\sin\theta$. To account for these approximations a correction term was added to the right-hand side of (21). This term includes the effects of $\partial^2\zeta/\partial\xi^2$ and the three terms in the expansion

$$\sin\theta = \sin(2\phi kz) \sim 2\phi kz - \frac{4}{3}\phi^3k^3z^3 + \frac{4}{15}\phi^5k^5z^5 \quad \text{for small } z$$

and is given by

$$\begin{aligned} C_n(z) = {} & -2k^2zg_n - \frac{5}{2}k^2zg_n' - \frac{1}{2}k^2z^3g_n'' \\ & - \sum_{i=1}^{\infty} k^2zg_i\left\{\frac{3}{2}\sqrt{2(i+1)}\int_{-\infty}^{\infty}\phi\mu_{i+1}\mu_n\,\mathrm{d}\phi + \frac{1}{3}\sqrt{2(i+1)}\int_{-\infty}^{\infty}\phi^3\mu_{i+1}\mu_n\,\mathrm{d}\phi\right. \\ & \qquad - (i+5)\int_{-\infty}^{\infty}\phi^2\mu_i\mu_n\,\mathrm{d}\phi + \frac{4}{3}k^2z^2\int_{-\infty}^{\infty}\phi^4\mu_i\mu_n\,\mathrm{d}\phi \\ & \qquad \left. + \frac{2}{5}\sqrt{2(i+1)}k^2z^2\int_{-\infty}^{\infty}\phi^5\mu_{i+1}\mu_n\,\mathrm{d}\phi\right\} \\ & - \sum_{i=1}^{\infty} k^2z^2g_i'\left\{\sqrt{2(i+1)}\int_{-\infty}^{\infty}\phi\mu_{i+1}\mu_n\,\mathrm{d}\phi + \frac{2}{3}k^2z^2\int_{-\infty}^{\infty}\phi^4\mu_i\mu_n\,\mathrm{d}\phi - 2\int_{-\infty}^{\infty}\phi^2\mu_i\mu_n\,\mathrm{d}\phi\right\} \end{aligned}$$

$$\text{for } n = 1, 2, \ldots. \qquad (57)$$

The inclusion of this correction renders the procedure essentially exact. It was observed that adding this term barely changed the results and thus justifies the approximations. Also, the various integrals appearing in (22), (49) and (57) involving Hermite polynomials all have exact solutions and can be found in Gradshteyn and Ryzhik [14]. All other integrals were evaluated numerically by Filon integration.

Comparisons of the present results with existing results in the literature are also made in Table 2. The agreement is quite good. Another comparison comes from the estimation of the critical Reynolds number, R_C, at which separation first sets in. This corresponds to the value of R which makes the sum

$$\sum_{n=1}^{N_0} nr_n(0)$$

vanish. The present method predicts the critical Reynolds number to lie in the range $6.37 \leqslant R_C \leqslant 6.38$ and agrees well with the value of 6.2 predicted by Dennis and Chang [6].

Numerical solutions for asymmetric flow past a rotating circular cylinder were also obtained for the Reynolds numbers $R = 5$ and 20 with rotation rates in the range $0 \leqslant \Omega \leqslant 0.5$. This problem was found to be much more sensitive than the symmetric case. The symmetric solution was used as the initial guess for small Ω which in turn was used as the initial guess for the next higher rotation rate. Stepping Ω in this manner accelerated the convergence of the numerical procedure. In all cases, the grid size $M \times N = 60 \times 80$, the relaxation parameter $\omega = 0.05$ and $\xi^* = 5$ (corresponding to approximately 150 radii) for $R = 5$ and 20 were found to be adequate. It was observed that attaching the outer region beyond the boundary $\xi = \xi^*$ had a negligible effect on the drag and lift coefficients. For the symmetrical case, the correction brought about by the addition of the outer region was of the order of 5%. Table 3 compares drag and lift coefficients obtained by the present method with the recent works of Badr et al. [15] and Ingham and Tang [16]. Good agreement is found for the various rotation rates and Reynolds numbers. In fact the results are identical to all figures quoted with those obtained by D'Alessio and Dennis [17] using a completely different model of the Navier–Stokes equations.

Young [10] scales the vorticity and stream function so that they are $O(1)$ in the far field. The asymptotic conditions of Imai are used at distances as far as 400 radii away. Ingham and Tang [16], on the other hand, also consider the entire flow field by using the transformation $\xi = 1/r$, which maps $r = \infty$ to $\xi = 0$. The function $f = \psi^*/r$ is used in place of the perturbed

Table 3. Comparison of C_L and C_D for the rotating circular cylinder with existing results

R	Ω	Badr, Dennis and Young (1989)		Ingham and Tang (1990)		Present	
		$-C_L$	C_D	$-C_L$	C_D	$-C_L$	C_D
5	0.1	0.285	3.92	0.277	3.947	0.266	3.896
	0.2	0.572	3.91	0.559	3.939	0.533	3.893
	0.4	1.14	3.90	1.111	3.927	1.068	3.884
	0.5	1.37	3.89	1.389	3.916	1.336	3.877
20	0.1	0.266	2.00	0.254	1.995	0.243	1.916
	0.2	0.552	2.00	0.514	1.992	0.486	1.915
	0.4	1.11	1.97	1.024	1.979	0.974	1.912
	0.5	1.39	1.97	1.283	1.973	1.220	1.910

stream function ψ^* and the conditions imposed on $\xi = 0$ (or $r = \infty$) are $f = 0$ and $\zeta = 0$. Both of these authors also use a local h^2-accurate formula to compute the surface vorticity.

As a final note concerning the results, various tests were performed on the solutions obtained. For example, $g_n(z = 0)$, $r_n(z = 0)$ and $F_n(z = 0)$ were calculated and compared against the theoretical values given by (23), (50) and (51), respectively. Also, the values of C_D and C_L for paths of integration near the cylinder surface were compared with those computed round large contours in the outer region. Lastly, for the case of asymmetric flow the periodicity of the surface pressure was also checked by investigating the difference $P_0(\pi) - P_0(-\pi)$. In all of these tests, the errors recorded were tolerable with the largest error of the order of 5%.

7. Conclusion

An important feature associated with this numerical method is worth pointing out. The solution in the outer region includes the effects of terms far beyond the range of the asymptotic solution of Imai [11], which could be used as an alternative at the boundary $\xi = \xi^*$. In fact, this method implicitly enforces the asymptotic condition at infinity, where it becomes exact. Hence, these solutions may be judged to be accurate and reliable. We note that there are many ways of approaching the problem of matching the two regions and this present paper makes a start in analysing the problem.

Calculations were not carried out to higher values of R because of poor convergence properties of the iterations, which may well be associated with the positioning of the boundary $\xi = \xi^*$. To proceed to higher Reynolds numbers would require finer grids in both the inner and outer regions as well as the perfection of some of the techniques used. Further, the substitution of another model for the inner region to better accommodate boundary-layer theory may be in order. Such a model has already been suggested by D'Alessio and Dennis [17]. Our main objective in this work is to propose a way of dealing with the structure of the outer solution via equation (13) and to offer a numerical method of implementing it. Also, it must be remembered that in practice steady-state flows past cylinders are limited to low Reynolds numbers beyond which vortex shedding takes place. Moreover, from the information gained in the present study it may well be possible to proceed to higher values of R, as Tang and Ingham [18] have certainly done in the case of flow past a rotating cylinder.

Lastly, we emphasize that this method applies to any cylinder cross section because it is based on boundary-layer theory and the asymptotic solution, both of which make no reference to a particular cross section. The circular cylinder was chosen as a trial case because of its relative simplicity and also because of the abundance of results existing in the literature available for comparison purposes. A similar type of method has been applied to determine the flow parallel to a finite flat plate for Reynolds numbers up to 200 which has succeeded in verifying the triple-deck structure at the trailing edge. We admit that the method does require extra programming, but the domain decomposition is important in recognizing the mathematical structure of the flow at large distances. It may be possible to apply the method in three-dimensions provided an appropriate co-ordinate expansion can be used since it depends, in effect, on a linearization of the equations of motion at large distances. There is also the possibility of linearizing turbulent flow once a turbulence model is given. All these questions are, however, dependent on future developments.

Acknowledgement

Financial support for this research was provided by the Natural Sciences and Engineering Research Council of Canada.

References

1. A. Thom, The flow past circular cylinders at low speeds. *Proc. Roy. Soc.* A 141 (1933) 651.
2. M. Kawaguti, Numerical solution of the Navier–Stokes equations for flow around a circular cylinder at Reynolds numbers 40. *J. Phys. Soc. Japan* 8 (1953) 747.
3. H.B. Keller and H. Takami, Numerical studies of viscous flow about cylinders. In: D. Greenspan (ed.), *Numerical Solutions of Nonlinear Differential Equations*. Wiley, New York (1966) p. 115.
4. H. Takami and H.B. Keller, Steady two-dimensional viscous flow of an incompressible fluid past a circular cylinder. *Phys. Fluids* Suppl. II (1969) 51.
5. S.C.R. Dennis and Gau-Zu Chang, Numerical integration of the Navier–Stokes equations in two-dimensions. Mathematics Research Center, University of Wisconsin. *Technical Summary Report* #859 (1969).
6. S.C.R. Dennis and Gau-Zau Chang, Numerical solutions for steady flow past a circular cylinder at Reynolds numbers up to 100. *J. Fluid Mech.* 42 (1970) 471.
7. F. Nieuwstadt and H.B. Keller, Viscous flow past circular cylinders. *Comp. Fluids* 1 (1973) 59.
8. S.C.R. Dennis, A numerical method for calculating steady flow past a cylinder. In: A.I. Van de Vooren and P.J. Zandbergen (eds), *Proc. 5th Int. Conf. on Numerical Methods in Fluid Dynamics. Lecture Notes in Physics* 59 (1976) 165.
9. B. Fornberg, A numerical study of steady viscous flow past a circular cylinder. *J. Fluid Mech.* 98 (1980) 819.
10. P.J.S. Young, Steady asymmetric flow of a viscous fluid past a cylinder. Ph.D. Thesis, University of Western Ontario, London, Ontario, Canada (1989).
11. I. Imai, On the asymptotic behaviour of viscous fluid flow at a great distance from a cylindrical body, with special reference to Filon's Paradox. *Proc. Roy. Soc. Lond.* A208 (1951) 487.
12. S.C.R. Dennis, A numerical method for calculating two-dimensional wakes. AGARD Conference Proceedings #60 on Numerical Methods for Viscous Flows (1967).
13. S.C.R. Dennis, The numerical solution of the vorticity transport equation. In: H. Cabannes and R. Temam (eds), *Proc. 3rd Int. Conf. on Numerical Methods in Fluid Dynamics. Lecture Notes in Physics* 19 (1973) 120.
14. I.S. Gradshteyn and I.M. Ryzhik, *Tables of Integrals, Series, and Products*. 4th ed. Academic Press Inc., New York (1965).
15. H.M. Badr, S.C.R. Dennis and P.J.S. Young, Steady and unsteady flow past a rotating circular cylinder at low Reynolds numbers. *Comp. Fluids* 17 (1989) 579.
16. D.B. Ingham and T. Tang, A numerical investigation into the steady flow past a rotating circular cylinder at low and intermediate Reynolds numbers. *J. Comp. Phys.* 87 (1990) 91.
17. S.J.D. D'Alessio and S.C.R. Dennis, A vorticity model for viscous flow past a cylinder. *Comp. Fluids* 23 (1994) 279.
18. T. Tang and D.B. Ingham, On steady flow past a rotating circular cylinder at Reynolds numbers 60 and 100. *Comp. Fluids* 19 (1991) 217.